RSC Advances

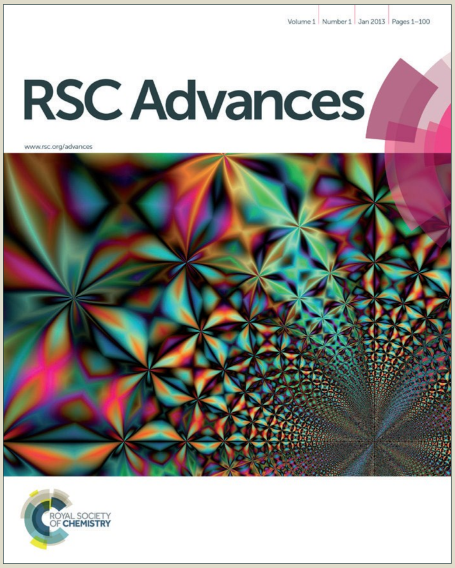

ROYAL SOCIETY OF CHEMISTRY

www.rsc.org/advances

Journal Name

ARTICLE

Highly effective chemosensor of luminescent silica@lanthanide complex@MOF heterostructure composite for metal ion sensing

Received 00th January 20xx,
Accepted 00th January 20xx

DOI: 10.1039/x0xx00000x

www.rsc.org/

Chang Liu, Bing Yan *

Heterostructure chemosensors have excellent chemical stability, low contaminativity and excellent recyclability, which are regarded as promising a new generation sensors with critical aspects to be related to the sensing sensitivity and selectivity of hetero-sensors. Our preparation strategy of the heterostructure sensors are constructed by luminescent lanthanide complexes and metal organic frameworks (MOF). The heterogeneous sensors are systematically produced by EuTTA and ZIF-8 to cover silica respectively, and thin particles obtained with small size and uniform morphology. Then, the particles are used to detect of Cu^{2+} in aqueous solution as a highly selective and sensitive sensor. Eventually, we found that the well-structured silica@EuTTA@ZIF-8 microspheres have good fluorescence stability, low detection limit and broad linear range in aqueous environment. Those excellent properties make the chemosensor for sensing of Cu^{2+} potentially in environmental or biological solution systems.

Introduction

The photoluminescent lanthanide coordination compounds have been fascinating by the researchers for many years for the effective energy transfer process from organic ligands to the lanthanide ions [1,2]. Unfortunately, lanthanide complexes themselves are still restricted to be really utilized in practical fields for their poor thermal and mechanical stability. Therefore, lanthanide complexes can be linked to inorganic or organic polymeric hosts through the physical doping or chemical bonding approaches [3,4], resulting in all kinds of lanthanide hybrid materials [5,6]. These hybrids can display favourable luminescent behaviour such as long lifetime and high internal quantum efficiency, which can be expected to have potential application in optical devices [7].

To presence, the host units for luminescent lanthanide hybrid materials involve sol-gel derived silica, mesoporous silica and microporous zeolite, organic polymers [8-11]. Besides, to overcome the shortcoming of the non-crystalline state hybrids, inorganic crystalline units are introduced to further improve the physical and chemical property of them. For example, all kinds of inorganic semiconductor inorganic nanocrystals or polyoxmetallate species are assembled with lanthanide complexes in the same hybrid system [12,13]. Some hybrid systems can be further realized luminescent tuning and integrating [14].

Metal–organic frameworks (MOFs) belong to crystalline hybrids by coordination reaction of metal ions and organic ligands [15], whose large specific surface area, ordered crystalline structure, and highly regular pores make them have a lot of potential applications such as gas storage, separations, ion exchange, catalysis and sensing, *etc.* [16] Zeolitic imidazolate frameworks (ZIFs) are a kind of MOFs comprised of tetrahedrally-coordinated transition metal ions connected by organic imidazole ligands, which are topologically isomorphic with zeolites [17]. Among ZIF-8 ($Zn(MeIM)_2$, MeIM = 2-methylimidazole) is a kind of chemically robust and thermally stable material and possesses the sodalite zeolite-type structure with large cavities and small pore apertures [18]. ZIF-8 is suitable host to compose all kinds of nanoparticles for its intersecting three-dimensional structural feature, high thermal stability, large pore size and surface area [19].

Considering the versatile chemical modification, different host units can be further assembled together. In fact, some works have been tried to compose MOFs and other host units [20]. On the other hand, MOFs are utilized to construct nanocomposite or nanostructure [21]. For ZIF-8, we have tried the assembly of it with other functional units to form the hybrid systems, involving in upconversion nanocrystal, polyometallate and complex species [22]. The different luminescent centers in these hybrids produce the multi-color luminescence and white luminescence under selected excitation. It is worthy pointing out that coordination polymers can be immobilized onto the carboxylate-terminated silica particles, resulting in the formation of novel silica@coordination polymer heterostructures [23]. This methodology provides a path for the in-situ immobilization of organic molecules to form coordination polymer and further preparation of heterostructure composite with silica, which can be expected to be utilized in many applications.

In this paper, new composite with silica@lanthanide complex@MOF heterostructure are designed and prepared and the synthetic progress was shown in scheme 1. The detailed physical

---

Department of Chemistry, Tongji University, Shanghai 200092, P. R. China. Email: byan@tongji.edu.cn.

† Electronic supplementary information (ESI) available: Experimental, synthesis and characterization details. See *DOI: 10.1039/x0xx00000x*

characterization and especially luminescent performance and sensing property are studied.

Experimental

Chemicals

All reagents were obtained from commercial sources (Sinoreagent, Sigma Aldrich, Aladdin) and were used without further purification unless otherwise stated. All of the metal ions aqueous solutions (Cd^{2+}, Ca^{2+}, Ni^{2+}, Fe^{3+}, Hg^{2+}, Pb^{2+}, Co^{2+}, Fe^{2+} and Cu^{2+}) were prepared from there nitrate salts. Europium chlorides were prepared by dissolving the corresponding oxides (Eu_2O_3) in excess hydrochloric acid (37 %) followed by evaporation and crystallization.

Surface carboxyl modified SiO_2 microspheres

The equal molar ratio of 3-triethoxysilylpropylamine (APTES) and succinic anhydride was dispersed uniformly in a certain amount of DMF with magnetic stirring 3 h under room temperature (25 °C). Then 20 mL DMF suspension of silica after ultrasonic dispersion and 2ml of deionized water were dropped into the above solution respectively, and continued magnetic stirring 5h at the same temperature. The nano-silica was isolated by ultrahigh-speed centrifuge, washed by alcohol several times, and the carboxylated modified SiO_2 spheres obtained.

Preparation of luminescent SiO_2@EuTTA microspheres

Solution A：$EuCl_3 \cdot 6H_2O$ (0.3662 g) was mixed with carboxylic acid-terminated silica (1.0 g) in 5 mL of water. Solution B：2-thenoyltrifluoroacetone (HTTA, 0.6664 g, 3 mmol) was dissolved in 10 mL of ethanol and NaOH aqueous solution (5 % w/v) was used to adjust the pH of this solution to 6.0. The protonated solution B was added dropwise to the aqueous solution A of Eu^{3+} and silica. After addition of 100 mL of water, the mixture was vigorous stirred for 120 min at 60 °C, and luminescent SiO_2@EuTTA microspheres generated. The microspheres were isolated by cooling the reaction mixture to room temperature, collecting the precipitate through centrifugation, and washing the precipitate several times with deionized water and dried in desiccators at room temperature.

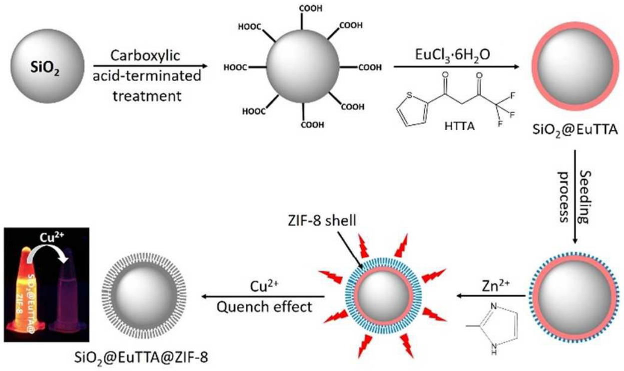

Scheme 1 Schematic representation for the synthetic progress of SiO_2@EuTTA@ZIF-8 and the fluorescent quenching phenomenon of Cu^{2+} to SiO_2@EuTTA@ZIF-8.

Synthesis of luminescent SiO_2@EuTTA@ZIF-8

Seeding process: An “In-situ” seeding process was developed as follows. 0.1 g of SiO_2@EuTTA spheres were added to a solution of 0.195 g $Zn(NO_3)_2 \cdot 6H_2O$ and 1.3 g H_2O, and sonicated for 5 min. Another 0.1 g of SiO_2@EuTTA was added into a solution of 3.78 g 2-methylimidazole and 13.3 g of H_2O, and sonicated for same time. Then the Zn^{2+} solution was dropped into the 2-methylimidazole solution under stirring for 5 min. The product was collected by centrifuging, washing 3 times with deionized water and dried overnight.

Regrowth of seeded SiO_2@EuTTA: 0.47 g $Zn(NO_3)_2 \cdot 6H_2O$ was dissolved in 20 mL of MeOH and water (1:1 v/v). In addition, 1 g 2-methylimidazole was dissolved into 10 mL of MeOH with 0.14 g of “in situ” seeded SiO_2@EuTTA. The two solutions were sonicated for 5 min and then the Zn^{2+} solution was dropped into the 2-methylimidazole solution under strong stirring 2 h. After that, the final product SiO_2@EuTTA@ZIF-8 heterostructure composite was collected by centrifuging with deionized water and MeOH several times, dispersed in MeOH to separate the microspheres and dried overnight.

Luminescent measurements

The photoluminescence phenomena of SiO_2@EuTTA@ZIF-8 with different metal ions were studied at room temperature. For the properties of sensing with respect to various metal ions, the emulsion of SiO_2@EuTTA@ZIF-8/M^{n+} were obtained by diffusing a certain amount of SiO_2@EuTTA@ZIF-8 powder (3.0 mg) into deionized water solution (3.0 mL) of $M(NO_3)n$ (M^{n+} = Cd^{2+}, Ca^{2+}, Ni^{2+}, Fe^{3+}, Hg^{2+}, Pb^{2+}, Co^{2+}, Fe^{2+} and Cu^{2+}) under the concentrations of 10^{-2} M. Then the mixtures solutions were sonicated for 30 min to form various metal ion-incorporated suspensions for luminescent measurements. The every sample has the same width of the excitation slit and the emission slit under excitation wavelength of 396 nm.

Physical Measurements

Scanning electronic microscope (SEM) images were recorded with a Hitachi S-4800 with a cold field emission gun operating at 2 kV and 10 μA. Transmission electron microscopy (TEM) was proceed on a JEOL JEM-2010F electron microscope and manipulated at 200 kV. The crystalline phases of the products were determined by the powder X-ray diffraction (PXRD) patterns which were recorded at room temperature under ambient conditions with Bruker D8 VANDANCE X-ray diffractometer with CuKa radiation under 40 kV and 40 mA, the data were collected within the 2θ range of 5 - 60°. Thermal gravimetric analysis (TGA) were carried out on a STA 449C (Netzsch) system with a heating rate of 5 K min^{-1} from 40 °C temperature to 800 °C under nitrogen atmosphere in the Al_2O_3 crucibles. Fourier transform infrared (FTIR) spectra were measured within the range 4000−400 cm^{-1} on a Nexus 912 AO446 spectrophotometer using KBr pellets. Luminescence excitation and emission spectra of the samples are obtained on Edinburgh FLS920 spectrophotometer. Lifetime measurements were performed on an Edinburgh FLS920 phosphorimeter using a 450 W xenon lamp as excitation source. The data of lifetime is achieved from fitting the experiment luminescent decay.

Results and discussion

Characterization

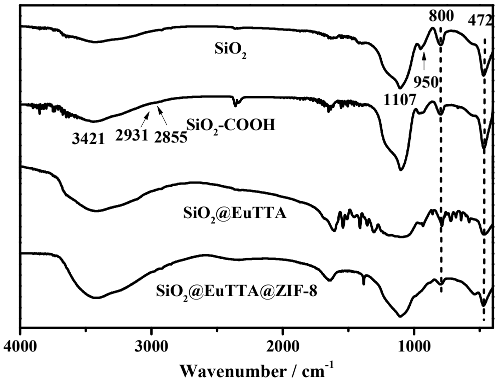

Fig. 1 FTIR spectra of the SiO$_2$ spheres, carboxylate terminated SiO$_2$ (SiO$_2$-COOH), SiO$_2$@EuTTA, and SiO$_2$@EuTTA@ZIF-8 heterostructure microspheres.

The carboxyl modification of the silica microspheres and the fabrication of the SiO$_2$@EuTTA@ZIF-8 heterostructure microspheres were characterized by FTIR spectra (Fig. 1,). The appearance of -COOH characteristic bands at 3500-2500 cm^{-1} and -CO-NH- at 1559 cm^{-1} demonstrates the successful carboxyl modification of silica spheres[24]. The increase of the peak intensity at 1107 cm^{-1} for Si-O-Si also confirms the condensation of (3-aminopropyl)triethoxysilane (APTES) with Si-OH[25]. The appearance of the characteristic bands of ZIF-8 for SiO$_2$@EuTTA@ZIF-8 heterostructure composite microspheres indicates the growth of ZIF-8 nanocrystals on the surface of the silica spheres. Moreover, the characteristic bands of silica at 800 and 472 cm^{-1} for carboxylate-terminated SiO$_2$, SiO$_2$@EuTTA and SiO2@EuTTA@ZIF-8 also reveal that the carboxyl modification, EuTTA and ZIF-8 growth did not affect the structure and composition of the core.

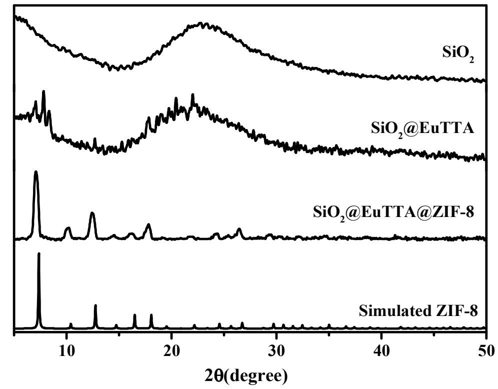

Fig. 2 PXRD patterns of SiO$_2$, SiO$_2$@EuTTA, SiO$_2$@EuTTA@ZIF-8 and simulated ZIF-8.

The PXRD patterns were further used to evaluate the composition of SiO$_2$@EuTTA@ZIF-8 (Fig. 2). The existence of the characteristic signal at 2θ=20–25° for SiO$_2$ and the characteristic peaks for ZIF-8 confirms the successful formation of the ZIF-8 layer on SiO$_2$@EuTTA microspheres. In the meantime, the peaks of SiO$_2$@EuTTA@ZIF-8 blanket the ground of SiO$_2$@EuTTA, which means that most of the SiO$_2$@EuTTA was dispersed into the inner of the layer.

Scanning electron microscope (SEM) and Transmission electron microscope (TEM) were used to monitor the fabrication of monodisperse SiO$_2$@EuTTA@ZIF-8 heterostructure composite microspheres. Fig. 3a and 3b were the SEM and TEM images of bare SiO$_2$ microsphere, and the diameter of particles were in the range of 100 to 110 nanometer. Selected SEM images and corresponding elemental mappings of SiO$_2$@ETTA and SiO$_2$@ETTA@ZIF-8 are shown in Figures S1 and S2. Comparison of the TEM images of SiO$_2$@EuTTA and SiO$_2$@EuTTA@ZIF-8 further demonstrates the ZIF-8 layer on the SiO$_2$@EuTTA core. ZIF-8 nanocrystals were observed on the surface of SiO$_2$@ETTA@ZIF-8 microspheres by controlling ZIF-8 growth (Fig. 3d). The diameter of SiO$_2$@EuTTA@ZIF-8 heterostructure composite microspheres increased from 130 mm for SiO$_2$@ETTA microspheres to 170 nm, thus indicating that a 20 nm thickness of ZIF-8 was grown on the SiO$_2$@ETTA microspheres.

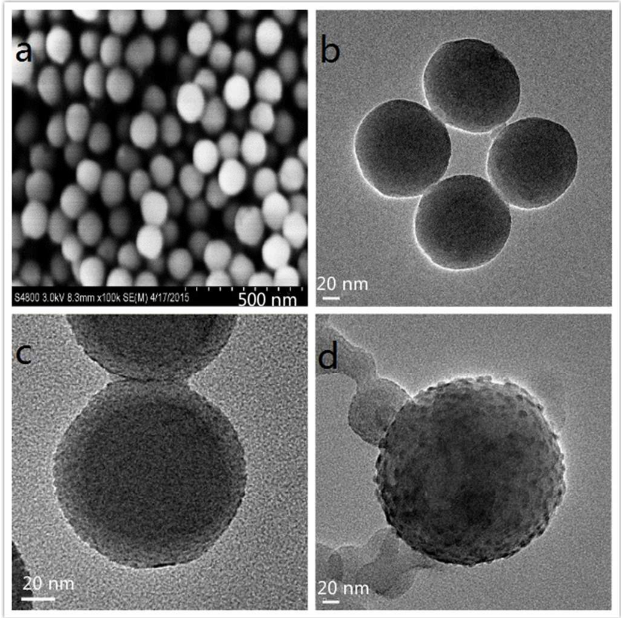

Fig. 3 SEM images: a) SiO$_2$; TEM images: b) SiO$_2$, C) SiO$_2$@EuTTA, and d) SiO$_2$@EuTTA@ZIF-8.

The thermal stability of the compounds is examined by thermal gravity analysis (TGA) measurements which is performed under air with a heating rate of 5 k·min^{-1} (Fig. S3). TGA data reveals that lanthanide complex start to release there coordinated organic molecules with the temperature rising from 25 ^{o}C. The SiO$_2$@EuTTA@ZIF-8 is stable up to 380 ^{o}C, which was much higher than for the synthesized SiO$_2$@EuTTA heterostructure microspheres (stable up to 200 ^{o}C). ZIF-8 also has the effect of protection for the core (SiO$_2$@EuTTA).

Luminescent properties

The photoluminescent spectra of SiO$_2$@EuTTA@ZIF-8 have been studied at room temperature. The fluorescence excitation and emission spectra of SiO$_2$@EuTTA@ZIF-8 show in Fig. 4. The excitation spectra is monitored by a sharp absorption band which is located in near ultraviolet region located at 396nm. The excitation spectra can indicate that the organic ligand can absorb the energy of near ultraviolet light efficiently and then sensitize the emission of Eu^{3+} by antenna effect. When the excited energy level of organic ligand is matched to the resonant excited levels of Eu^{3+} with a subsequent energy transfer, then SiO_2@EuTTA@ZIF-8 can obtain a final strong luminescence emission. Moreover, the emission spectra of SiO_2@EuTTA@ZIF-8 display the characteristic emission peaks of Eu^{3+} ion under an appropriate wavelength as the excitation source. The emission line of SiO_2@EuTTA@ZIF-8 was assigned to $^5D_0 \rightarrow {}^7F_0$, $^5D_0 \rightarrow {}^7F_1$, $^5D_0 \rightarrow {}^7F_2$, $^5D_0 \rightarrow {}^7F_3$ and $^5D_0 \rightarrow {}^7F_4$ transitions and the corresponding peaks are located at about 579, 591, 614, 651 and 701 nm, respectively. The emission peaks of SiO_2@EuTTA@ZIF-8 with different metal ions (Cd^{2+}, Ca^{2+}, Ni^{2+}, Fe^{3+}, Hg^{2+}, Pb^{2+}, Co^{2+}, Fe^{2+} and Cu^{2+}) are similar to that of the original which has the characteristic emission peak at about 614 nm under excitation wavelength of 396 nm.

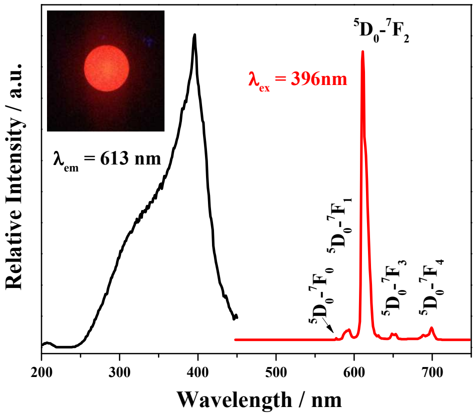

Fig. 4 Excitation and emission spectra of SiO_2@EuTTA@ZIF-8.

The pH-stability studies were used to test the fluorescent stability of samples under the change of pH values which were induced by various metal ions in solutions. The XRD patterns of SiO_2@EuTTA@ZIF-8 are almost unaltered in aqueous solutions, indicating that SiO_2@EuTTA@ZIF-8 can retain crystallinity and is stable in a wide pH range (Fig. S4)[26].The fluorescence intensity of SiO_2@EuTTA@ZIF-8 does not show obvious fluctuation when dispersed in different pH solutions (Fig. S5), the result indicates that SiO_2@EuTTA@ZIF-8 has excellent fluorescence stability and can be developed as a luminescent sensor for metal ions.

Sensing properties

The potential sensing of SiO_2@EuTTA@ZIF-8 for metal ions was examined as follows, a certain amount of SiO_2@EuTTA@ZIF-8 was dispersed into aqueous solutions containing different Cd^{2+}, Ca^{2+}, Ni^{2+}, Fe^{3+}, Hg^{2+}, Pb^{2+}, Co^{2+}, Fe^{2+} and Cu^{2+} ions. The luminescence of SiO_2@EuTTA@ZIF-8 solutions which were incorporated with metal ions was investigated. The photoluminescence intensity of SiO_2@EuTTA@ZIF-8 was relevant with the metal ion in aqueous (Fig. 5). When incorporated with the addition of Cu^{2+}, the luminescence intensity of SiO_2@EuTTA@ZIF-8 was decreased compared with others, the rest of metal ions (Cd^{2+}, Ca^{2+}, Ni^{2+}, Fe^{3+}, Hg^{2+}, Pb^{2+}, Co^{2+} and Fe^{2+}) have a negligible effect on the luminescence of Eu^{3+} in the aqueous solutions. Only Cu^{2+} could quench the red light emission and can be clearly seen under UV light excitation, the addition of other metal ions could not induce visible change in the inset of Fig. 5b. The microspheres have high selectivity for the specific recognition and sensing of Cu^{2+} in aqueous solutions. Table S1 showed the response of luminescence lifetime of SiO_2@EuTTA@ZIF-8 with various metal ions in aqueous solutions, respectively. The results indicate that most metal ions have a negligible effect on the emission lifetimes of SiO_2@EuTTA@ZIF-8. But the Cu^{2+}-incorporated SiO_2@EuTTA@ZIF-8 has a shorter emission lifetime than the original increasing from 590 µs to 12 µs, which is in agreement with the decrease of the luminescence intensity.

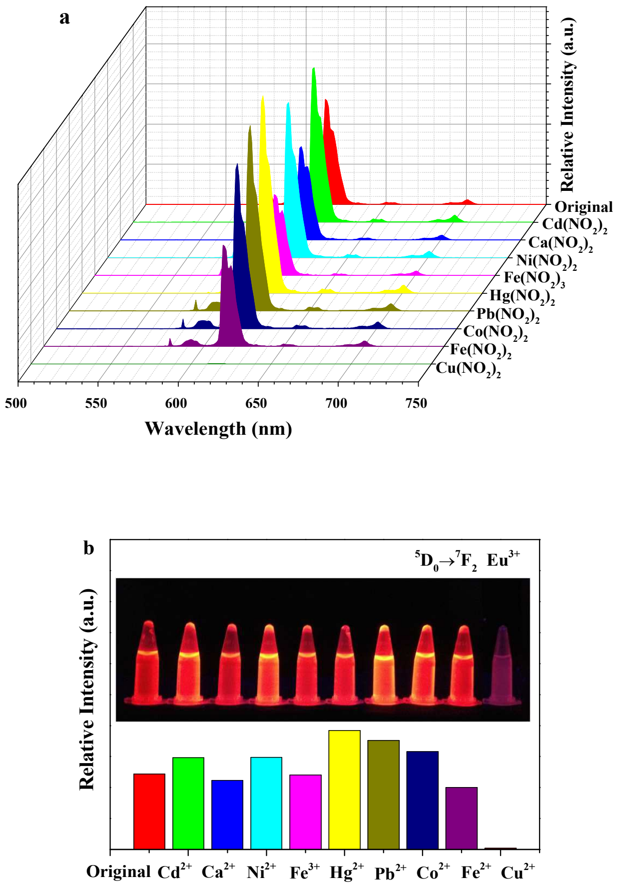

Fig. 5 (a) Suspension-state photoluminescent spectra and (b) the relative intensities of $^5D_0$ - $^7F_2$ at 613 nm for SiO_2@EuTTA@ZIF-8 dispersed in various metal ion aqueous solutions upon excitation at 396 nm. The inset is in the corresponding photographs under UV-light irradiation.

In Fig. 6, the compound SiO_2@EuTTA@ZIF-8 was immersed in different concentrations of Cu^{2+} for further luminescence studies. The luminescence intensity of SiO_2@EuTTA@ZIF-8 incorporated with Cu^{2+} shows a strong dependence on the concentration. The luminescence intensity decreases proportionally to the concentration of Cu^{2+}. The emission intensity of the SiO_2@EuTTA@ZIF-8 solution decreases sharply with the increase of

Cu^{2+} concentration from 0 to 500 μM. Quantitatively, this decrease effect can be rationalized by the Stern-Volmer equation:

$$I_0/I = 1 + K_{sv}[M]$$

The values of I_0 and I are the luminescence intensity of the SiO_2@EuTTA@ZIF-8 and SiO_2@EuTTA@ZIF-8/Cu^{2+}, respectively. K_{sv} is the decrease constant, [M] is the concentration of Cu^{2+}. The experimental data is the K_{sv} curve of SiO_2@EuTTA@ZIF-8 with Cu^{2+} illustrating in the inset of Fig. 6, and the linear correlation coefficient (R) is 0.99218, which suggests that the decrease effect of Cu^{2+} on the luminescence of SiO_2@EuTTA@ZIF-8 agrees the Stern-volmer mode well. The K_{sv} value is calculated as 3.144×10^4 M^{-1}, which reveals a strong decrease effect on the SiO_2@EuTTA@ZIF-8 luminescence.

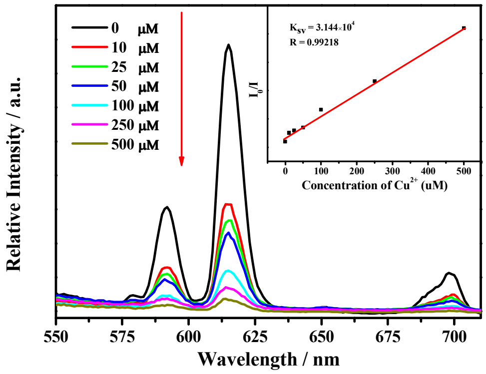

Fig. 6 Emission spectra of SiO_2@EuTTA@ZIF-8 in aqueous solutions in the presence of various concentrations of Cu^{2+} under excitation at 396 nm and the inset is the K_{sv} curve (linear relationship of the emission intensity) of SiO_2@EuTTA@ZIF-8 decreased by Cu^{2+} ions.

To examine the possible mechanism for the luminescence quenching effect by metal ions, O1s X-ray photoelectron spectroscopy studies are carried out on SiO_2@EuTTA@ZIF-8 and SiO_2@EuTTA@ZIF-8/Cd^{2+} (Fig. 7). The O 1s peak is shifted to 530.4 eV with the addition of Cu^{2+} comparing with SiO_2@EuTTA@ZIF-8 at 530.0 eV. There may be a weak coordination binding of uncoordinated carbonyl to Cu^{2+} in the SiO_2@EuTTA@ZIF-8/Cd^{2+}. Such coordination of Cu^{2+} ion can enhance various non-radiative activations and increase energy loss. This reduces the intraligand ligand-to-Eu energy transfer efficiency, and quenches Eu red light emissions. Time-Resolved fluorescence emission measurements are also used to further demonstrate the luminescence quenching effect of Cu^{2+}ion, and the response of luminescence lifetime was shown in Table S1. It is found that the Cu^{2+}-incorporated SiO_2@EuTTA@ZIF-8 has a shorter emission lifetime than SiO_2@EuTTA@ZIF-8, which is in agreement with the decrease of the photoluminscent intensity.

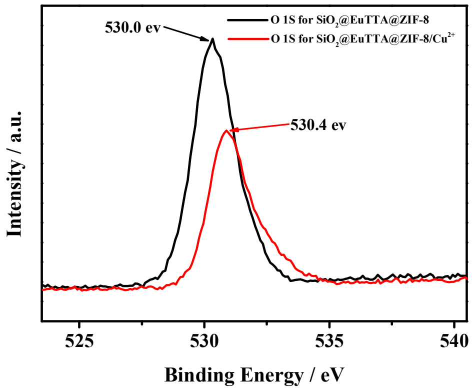

Fig. 7 XPS spectra of the original (black) and Cu^{2+}-incorporated (red) dispersed in 10^{-2} M H_2O solution of $Cu(NO_3)_2$, where the black curve denotes the O1s for SiO_2@EuTTA@ZIF-8 and red curve denotes the O1s for SiO_2@EuTTA@ZIF-8/Cu^{2+}.

At last, we have examined the recyclability of SiO_2@EuTTA@ZIF-8 microspheres for sensing processes. SiO_2@EuTTA@ZIF-8 microspheres can be reused several times by simply washing the chemsensors with fresh MeCN after the sensing process (Fig. 8).

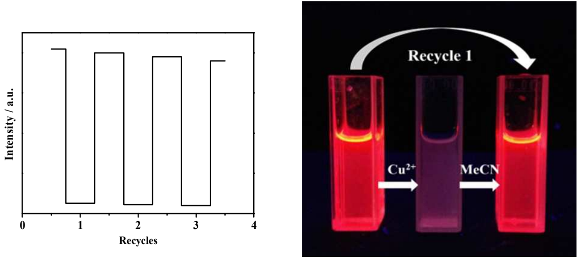

Fig. 8 a) On-off cycles of the SiO_2@EuTTA@ZIF-8 by alternating treatment of Cu^{2+} and MeCN at room temperature, b) photograph of SiO_2@EuTTA@ZIF-8 microspheres recycled 1 times for Cu^{2+} sensing.

Conclusions

In summary, the heterostructure sensors are constructed by luminescent lanthanide complexes (Eu-TTA) and metal organic frameworks (ZIF-8) to cover the core of silica. The thin heterostructure composite silica@EuTTA@ZIF-8 microspheres particles are used to detect of Cu^{2+} in aqueous solution as a highly selective and sensitive sensor, showing good fluorescence stability, low detection limit and broad linear range in aqueous environment. This makes the chemosensor for environment sensing of Cu^{2+} potentially for its excellent chemical stability, low contaminativity and excellent recyclability which are regarded as promising a new generation sensors.

Acknowledgements

This work is supported by the National Natural Science Foundation of China (21571142) and Developing Science Funds of Tongji University.

Notes and references

[a] Department of Chemistry, Tongji University; Siping Road 1239, Shanghai 200092, China. E-mail: byan@tongji.edu.cn

Electronic Supplementary Information (ESI) available: [details of any supplementary information available should be included here]. See DOI: 10.1039/b000000x/

1 (*a*) N. Sabbatini, M. Guardigli and J. M. Lehn, *Coord. Chem. Rev.*, 1993, **123**, 201; (*b*) T. Justel, H. Nikol and C. Ronda, *Angew. Chem. Int. Edi.*, 1998, **37**, 3085; (*c*) D. Parker, R. S. Dickins, H. Puschmann, C. Crossland and J. A. K. Howard, *Chem. Rev.*, 2002, **102**, 1977; (*d*) A. J. Kenyon, *Prog. Quantum Electron.*, 2002, **26**, 225.

2 (*a*) J. C. G. Bunzli, *Acc. Chem. Res.*, 2006, **39**, 53; (*b*) S. V. Eliseeva and J. C.G. Bunzli, *Chem. Soc. Rev.*, 2010, **39**, 189.

3 (*a*) P. A. Tanner, B. Yan and H. J. Zhang, *J. Mater. Sci.*, 2000, **35**, 4325; (*b*) B. Yan, *Mater. Lett.*, 2003, **57**, 2535; (*c*) B. Yan and Q. M. Wang, *Opt. Mater.*, 2004, **27**, 533.

4 (*a*) Q. P. Li and B. Yan, *J. Coll. Interf. Sci.*, 2012, **380**, 67; (*b*) Y. Y. Li and B. Yan, Dalton Trans., *2013*, **42**, 1678.

5 (*a*) L. D. Carlos, R. A. S. Ferreira, V. D. Bermudez and S. J. L. Ribeiro, *Adv. Mater.*, 2009, **21**, 509; (*b*) K. Binnemans, *Chem. Rev.*, 2009, **109**, 4283.

6 (*a*) B. Yan, *RSC Adv.*, 2012, **2**, 9304; (*b*) J. Feng, H. J. Zhang, *Chem. Soc. Rev.*, 2013, **42**, 387.

7 L. D. Carlos, R. A. S. Ferreira, V. D. Bermudez, B. Julian-Lopez and P. Escribano, *Chem. Soc. Rev*., 2011, **40**, 536.

8 (*a*) A. C. Franville, D. Zambon and R. Mahiou, *Chem. Mater.*, 2000, **12**, 428; (*b*) H. R. Li, J. Lin, H. J. Zhang, H. C. Li, L. S. Fu and Q. G. Meng, *Chem. Commun.*, 2001, 1212; (*c*) Q. M. Wang, and B. Yan, *J. Mater. Chem.*, 2004, **14**, 2450; (*d*) B. Yan and Q. M. Wang, *Cryst. Growth Des.*, 2008, **8**, 1484; (*e*) B. Yan and H. F. Lu, *Inorg. Chem.*, 2008, **47**, 5601.

9 (*a*) Y. Wang, H. R. Li, Y. Feng, H. J. Zhang, G. Calzaferri and T. Z. Ren, *Angew. Chem. Int. Ed.*, 2010, **49***,* 1434; (*b*) P. P. Cao, Y. G. Wang, H. R. Li and X. Y. Yu, J. Mater. Chem., 2011, **21**, 2709; (*c*) J. N. Hao and B. Yan, *Dalton Trans.*, 2014, **43**, 2810; (*d*) L. Chen and B. Yan, *Dalton Trans.*, 2014, **43**, 14123.

10 (*a*) L. N. Sun, H. J. Zhang, L. S. Fu, F. Y. Liu, Q. G. Meng, C. Y. Peng and J. B. Liu, *Adv. Funct. Mater.*, 2005, **15**, 1041; (*b*) X. M. Guo, H. D. Guo, L. S. Fu, R. P. Deng, W. Chen, J. Feng, S. Dang and H. J. Zhang, *J. Phys. Chem. C*, 2009, **113**, 2603.; (*c*) Y. Li, B. Yan and Hong Yang, *J. Phys. Chem. C*, 2008, **112**, 3959; (*d*) Y. J. Li, L. Wang and B. Yan, *J. Mater. Chem*., 2011, **21**, 1130.

11 (*a*) B. Yan and X. F. Qiao, *J. Phys. Chem. B*, 2007, **111**, 12362; (*b*) X. F. Qiao and B. Yan, *J. Phys. Chem. B*, 2008, **112**, 14742. (*c*) X. F. Qiao and B. Yan, *J. Phys. Chem. B*, 2009, **113**, 11865; (*d*) D. M. Wang. J. H. Zhang, Q. Lin, L. S. Fu, H. J. Zhang and B. Yang, *J. Mater. Chem.*, 2003, **13**, 2279.

12 (*a*) B. H. Kwon, H. S. Jang, H. S. Yoo, S. W. Kim, D. S. Kang, S. Maeng, D. S. Jang, H. Kimand D. Y. Jeon, *J. Mater. Chem.*, 2011, **21**, 12812; (*b*) Y. Zhao and B. Yan, *Dalton Trans.*, 2012, **41**, 5334; (*c*) Y. Zhao and B. Yan, *J. Coll. Interf. Sci.*, 2013, **395**, 145; (*d*) Q. P. Li and B. Yan, *RSC Adv.*, 2012, **2**, 10840.

13 (*a*) J. Cuan and B. Yan, *Dalton Trans.*, 2013, **43**, 14230; (*b*) J. Cuan and B. Yan, *RSC Adv.*, 2013, **3**, 20077; (*c*) J. Cuan and B. Yan, *RSC Adv.*, 2014, **4**, 1735; (*a*) J. Cuan and B. Yan, *Dalton Trans.*, 2013, **43**, 14230.

14 (*a*) Y. Mei and B. Yan, *New J. Chem.*, 2013, **37**, 2619; (*b*) T. W. Duan and B. Yan, *CrystEngComm*, 2014, **16**, 3395.

15 (*a*) M. Kurmoo, *Chem. Soc. Rev.,* 2009, **38**, 1353; (*c*) S. Natarajan and P. Mahata, *Chem. Soc. Rev.*, 2009, **38**, 2304; (*c*) O. Shekhah, J. Liu, R. A. Fischer and C. Woll, *Chem. Soc. Rev.*, 2011, **40**, 1081; (*d*) A. Betard and R. A. Fischer, *Chem. Rev.*, 2012, **112**, 1055.

16 (*a*) J. J. Perry IV, J. A. Perman and M. J. Zaworotko, *Chem. Soc. Rev.*, 2009, **38**, 1400; (*b*) D. Zhao, D. J. Timmons, D. Q. Yuan and H. C. Zhou, *Acc. Chem. Res.*, 2011, 44, 123; (*c*) M. O'Keeffe, O. M. Yaghi, *Chem. Rev.*, 2012, **112**, 675; (*d*) F. A. Almeida Paz, J. Klinowski, S. M. F. Vilela, J. P. C. Tome, J. A. S. Cavaleiro and J. Rocha, *Chem. Soc. Rev.*, 2012, **41**, 1088.

17 (*a*) O. M. Yaghi, M. O'Keeffe, N. W. Ockwig, H. K. Chae and M. Eddaoudi, J. Kim, *Nature*, 2003, **423**, 705; (*b*) H. Hayashi, A. P. Cote, H. Furukawa, M. O'Keeffe and O. M. Yaghi, *Nat. Mater.*, 2007, **6**, 501; (*c*) X. C. Huang, Y. Y. Lin, J. P. Zhang and X. M. Chen, *Angew. Chem., Int. Ed.*, 2006, **45**, 1557.

18 (*a*) J. Cravillon, S. Münzer, S. J. Lohmeier, A. Feldhoff, K. Huber, M. Wiebcke, *Chem. Mater.*, 2009, **21**, 1410; (*b*) H. Bux, F. Y. Liang, Y. S. Li, J. Cravillon, M. Wiebcke and J. Caro, *J. Am. Chem. Soc.* 2009, **131**, 16000; (*c*) S. R. Venna, M. A. Carreon, *J. Am. Chem. Soc.*, 2010, **132**, 76.

19 (*a*) R. Ostermann, J. Cravillon, C. Weidmann, M. Wiebcke and B. M. Smarsly, *Chem. Commun.*, 2011, **47**, 442; (*b*) J. F. Yao, D. H. Dong, D. Li, L. He, G. S. Xu and H. T. Wang, *Chem. Commun.*, 2011, **47**, 2559; (*c*) G. Lu, S. Z. Li, Z. Guo, O. K. Farha, B. G. Hauser, X. Y. Qi, Y. Wang, X. Wang, S. Y. Han, X. G. Liu, J. S. DuChene, H. Zhang, Q. C. Zhang, X. D. Chen, J. Ma, S. C. J. Loo, W. D. Wei, Y. H. Yang, J. T. Hupp, F. W. Huo, *Nat. Chem.*, 2012, 4, 310; (*d*) W. W. Zhan, Q. Kuang, J. Z. Zhou, X. J. Kong, Z. X. Xie, L. S. Zheng, *J. Am. Chem. Soc.*, 2013, **135**, 1926.

20 X. Lian and B. Yan, *New J. Chem.*, 2015, **39**, 5898.

21 (*a*) A. S. Huang, H. Bux, F. Steinbach and J. Caro, *Angew. Chem. Int. Ed.*, 2010, **49**, 4958; (*b*) A. S. Huang and J. Caro, *Angew. Chem. Int. Ed.*, 2011, **50**, 4979; (*c*) A. S. Huang, N. Y. Wang, C. L. Kong and J. Caro, *Angew. Chem. Int. Ed.*, 2012, **51**, 10551.

22 (*a*) C. Liu and B. Yan, *Eur. J. Inorg. Chem.*, 2015, 279; (*b*) C. Liu and B. Yan, *RSC Adv.*, 2015, **5**, 11101; (*a*) C. Liu and B. Yan, *New J. Chem.*, 2015, **39**, 112.

23 C. Jo, H. J. Lee and M. Oh, *Adv. Mater.*, 2011, **23**, 1716.

24 D. J. Macquarrie, *Chem. Commun.*, 1996, 1961.

25 Q. P. Liu, L. X. Gao, Z. W. Gao, L. Yang, Mater. Lett. 2007, **61**, 4456.

26 Q. P. Li, Z. L. Yuan, J. J. Qian and S. W. Du, *Rsc Adv.*, 2015, **5**, 49110.